J. Biomed. Eng. Res.
Vol.26, No.1, 31-35, 2005

A Synthetic Aperture Focusing Method for Three-way Dynamic Focusing

Jung-Jun Kim, Jin-Ho Chang, Tai-Kyong Song

Department of Electronics, Sogang University
(Received October 24, 2004. Accepted November 17, 2004)

Abstract: A novel synthetic aperture method for real-time three-way dynamic focusing is proposed, which provides lateral beam patterns represented as the product of Fourier transforms of transmit subaperture, receive subaperture, and a synthetic window function. In the proposed method, all array elements are fired individually and for each firing echo signals are recorded from all elements of a receive subaperture moving along an array with the transmit element. The three-way dynamic focusing is then achieved by employing a synthetic aperture algorithm for two-way dynamic focusing and a synthetic focusing method for transmit dynamic focusing. Both theoretical analysis and computer simulation results show that the proposed method produces ultrasound beams with improved lateral resolution at all depths compared to the conventional phased array imaging and synthetic aperture focusing methods.

Key words: Medical ultrasound imaging, Synthetic aperture, Ultrasound focusing

INTRODUCTION

Receive dynamic focusing based on digital beamforming methods has known to be the most successful approach to improve the lateral resolution in real-time ultrasound phased array imaging. The lateral resolution can be further improved by employing two-way dynamic focusing. Synthetic focusing (SF) is one of the methods that can achieve two-way dynamic focusing, in which all elements of each subaperture are fired successively, one at a time [1]. Since this data acquisition process must be repeated for all scan lines with different subapertures, the resulting frame rate will be impractically low.

Synthetic aperture focusing (SAF) is another method to achieve two-way dynamic focusing. In most SAF methods for two-way dynamic focusing (SAF-2W), spherical waves are transmitted either with a single element or with a virtual source element and echo signals are recorded individually from all elements of a receive subaperture, with both the transmit element and receive subapertures being stepped across an array in a succession of firings [2]-[7]. Each scan line is then obtained by properly combining the adjacent scan line data. Since the number of firings to form a single image frame is usually the same as the number of scan lines per image frame, frame rate is not sacrificed in the SAF systems. Fourier transform theory indicates that in lossless homogeneous media two-way focusing can be achieved through one-way focusing with an effective aperture [7], defined as the convolution of the transmit and receive aperture functions. In tissue-like media, however, the focused beam pattern is no longer represented as the Fourier transform of an associated aperture due to some waveform distortion effects, including phase aberrations [8],[9]. These inhomogeneities introduce focusing delay errors that deteriorate the lateral beam pattern, often resulting in high sidelobe levels. For this reason, in practical imaging, two-way focusing with an actual aperture is preferred to one-way focusing with an effective aperture.

In this paper, we propose a SAF method for three-way dynamic focusing (SAF-3W), which combines transmit dynamic focusing and SAF-2W techniques. It will be shown theoretically that the resulting lateral beam pattern is represented as the product of Fourier transforms of three functions: transmit and receive subaperture functions, and a synthetic window function that specifies the range of transmit subapertures used to form a synthesized beam along each scan line. Since this three-way focusing is achieved without using an effective aperture, the SAF-3W will provide better lateral resolution than the SAF-2W methods in practical imaging. We will also present a real-time data acquisition method for transmit dynamic focusing so that SAF-3W can be

Corresponding Author: Tai-Kyong Song
K235 SOGANG UNIV. ShinSu-Dong 1, MaPo-Gu, SEOUL, KOREA
Tel. 02-705-8907 Fax. 02-707-3008
E-mail. tksong@sogang.ac.kr

implemented with no decrease in frame rate compared to the conventional phased array (PA) imaging. In this method, each array element is fired only once and the returned ultrasound signals are received with a receive subaperture with twice more elements than needed to produce the same beam patterns when real-time imaging is not required. Computer simulation results show that SAF-3W provides better lateral beam patterns than PA and SAF-2W when they are implemented with the same number of active channels on both transmit and receive.

THEORY AND DATA ACQUISITION SCHEME

In an array imaging system with N parallel active array channels, a subaperture consisting of N array elements is stepped across an array to scan an area of interest, with both the transmitted and received ultrasound waves being focused along the center axis of each subaperture. Fig. 1 shows a subaperture A_i, which consists of N (=$2M$+1) elements and is centered at $x = i \cdot d$, with d being the inter-element spacing. Now suppose that I(=$2L$+1) subapertures ($A_i, -L \le i \le L$) are focused at z=F on the z-axis, on both transmit and receive. Summing the focused signals from these subapertures with delays, $\exp\{-jk(id)^2/2F\}$, to compensate the different transmit path delays between the focal point and subaperture centers, one can obtain the continuous wave angular point spread function (PSF),

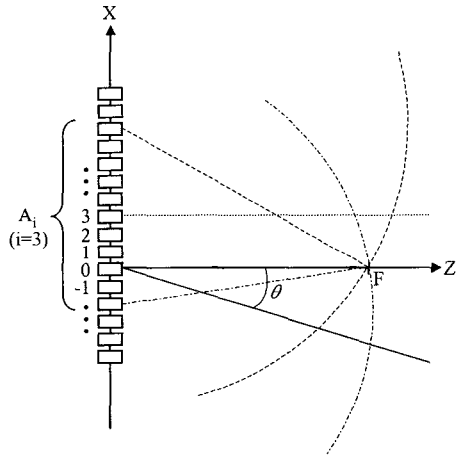

Fig. 1. Illustration of the data acquisition stratages for three-way dynamic focusing. All the relevant subapertures ($A_i, -L \le i \le L$) are focused at the imaging point X=0,Z=F) on a scan line (Z-axis in this case) on both transmit and receive. The focused signals of all the subapertures are summed to form the imaging point.

$$\Psi_{SAF-3W}(\theta) \propto \sum_{i=-L}^{L}\left\{\sum_{m=i-K}^{i+K} e^{-jkx_m \sin\theta}\right\}\cdot\left\{\sum_{n=i-M}^{i+M} e^{-jkx_n \sin\theta}\right\} \quad (1)$$

$$= \sum_{i=-L}^{L} e^{-jk2di\sin\theta\cdot i} \cdot \sum_{m'=-K}^{K} e^{-jkd\sin\theta\cdot m'} \cdot \sum_{n'=-M}^{M} e^{-jkd\sin\theta\cdot n'} \quad (2)$$

$$\propto \frac{\sin(k\sin\theta\cdot Id)}{\sin(k\sin\theta\cdot d)} \times \left\{\frac{\sin(k\sin\theta\cdot Nd/2)}{\sin(k\sin\theta\cdot d/2)}\right\}^2 \quad (K=M) \quad (3)$$

where θ is the angle from the array normal, $x_m = md$ and $x_n = nd$ represent the center locations of the transmit and receive elements, respectively, and $k = 2\pi/\lambda$. Note that the number of transmit and receive elements used for beam synthesis in (1) are $2K$+1 and $2M$+1, respectively. The first term in (3) represents the Fourier transform of a function $A_S(i)$, which will be called a synthetic window function (SWF): in this case $A_S(i) = 1$ for $-L \le i \le L$ and 0 elsewhere. The second term represents the two-way focused angular PSF of the center subaperture A_0. Consequently, (3) represents the three-way (dynamically focused) beam pattern for K=M, which can be obtained only at the transmit focal depth (z=F).

To achieve three-way focusing at all depths, all the I subapertures must be focused dynamically on transmit. A straightforward approach to transmit dynamic focusing requires $I \cdot N_I \cdot N_S$ transmit-receive (T/R) steps to form a single image frame consisting of N_S scan lines and N_I imaging points on each scan line. The T/R steps for transmit dynamic focusing can be reduced to $N \cdot N_S$ by employing a SF scheme as illustrated in Fig. 2(a), where $I = 3$ and $N = 5$ for simplicity. But, the number of T/R steps is still N_S times larger than that of a conventional PA imaging. Fig. 2(b) shows the proposed data acquisition scheme for real-time SAF-3W, which only requires $N_S + 2M$ T/R steps. In Fig. 2(a), each element is fired N times, since it belongs to N adjacent transmit subapertures, and for each firing N elements are used for receiving echo signals. In Fig. 2(b), on the other hand, every element is fired

only once and $2N-1$ elements are used for signal reception in each T/R event. Since the transmitted signals from each element are received at $2N-1$ elements in Fig. 2(a), all the data sets from the entire T/R steps in Fig. 2(a) can be obtained from the T/R steps in Fig. 2(b). This implies that dynamically focused transmit beams along all scan lines can be produced with N_S+2M T/R steps. Summarizing, the three-way beam pattern in (3) can be obtained at all imaging points with the proposed data acquisition scheme with no sacrifice in the imaging frame rate compared to the conventional PA imaging.

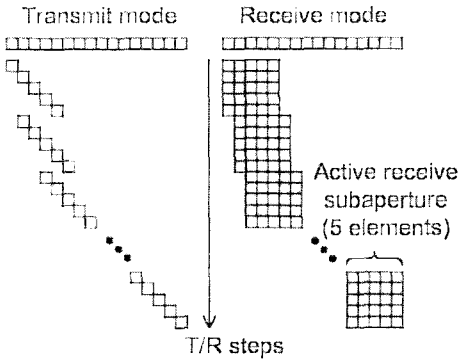

(a) A total of T/R steps are 60 times.

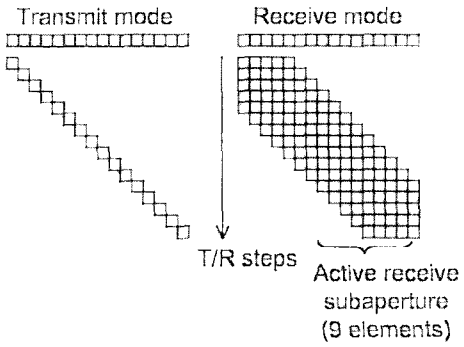

(b) A total of T/R steps are 16 times

Fig. 2. Transmit-receive steps for the realization of three-way dynamic focusing:(a) SF-based scheme for transmit dynamic focusing and (b) its modification for real-time data acquisition.

COMPARISON WITH OTHER METHODS

The real-time SAF-3W scheme (abbreviated to SAF-3W hereafter) uses $2N-1$ parallel active array channels to provide the angular PSF in (3). In this section, the SAF-3W will be compared to PA(RA), PA(TA), SAF-2W(RA), and SAF-2W(TA), where RA and TA in the parentheses represent the types of receive subapertures used for each method: RA and TA stand for rectangular and triangular apertures, respectively. Note that the effective aperture for rectangular transmit and receive apertures is expressed as a triangular function. All these methods are to be implemented using the same SWF and transmit subaperture, both of which are rectangular and encompass exactly N elements, and $2N-1$ active receive channels.

It is easy to show that the angular PSFs of these methods can be expressed as follows [10]:

$$\Psi_{PA(RA)}(\theta) \propto \frac{\sin^q(k\sin\theta\cdot Nd/2)}{\sin^q(k\sin\theta\cdot d/2)} \cdot \frac{\sin(k\sin\theta\cdot(2N-1)d/2)}{\sin(k\sin\theta\cdot d/2)} \tag{4}$$

$$\Psi_{PA(TA)}(\theta) \propto \frac{\sin^q(k\sin\theta\cdot Nd/2)}{\sin^q(k\sin\theta\cdot d/2)} \cdot \frac{\sin^2(k\sin\theta\cdot Nd/2)}{\sin^2(k\sin\theta\cdot d/2)} \tag{5}$$

$$\Psi_{SAF-2W(RA)}(\theta) \propto \frac{\sin(k\sin\theta\cdot Id)}{\sin(k\sin\theta\cdot d)} \cdot \frac{\sin(k\sin\theta\cdot(2N-1)d/2)}{\sin(k\sin\theta\cdot d/2)} \tag{6}$$

where $q=1$ for z=F and 0 for $|z-F|>>1$. Note that (4) and (6) can be obtained by substituting $L=0$ and $K=0$ in (1), respectively. (5) can simply be obtained from (4), according to the definition of an effective aperture. In both PA and SAF-2W methods, better resolution can be obtained with the RA scheme since two-way focusing with an aperture of size Nd produces much smaller sidelobe levels than one-way focusing with an effective aperture of size $(2N-1)d$.

In the same way to obtain (5) from (4), the angular PSF of SAF-2W(TA) in a lossless homogeneous medium can be obtained from (6), which will be exactly the same as that of SAF-3W in (3): but higher SNRs will be obtained with SAF-3W. In tissue-like media, however, phase aberrations caused by spatial inhomogeneities in the acoustic velocity introduce focusing delay errors, resulting in the elevation of sidelobe levels. Therefore, product of two deteriorated focused beams will exhibit lower sidelobe levels. Consequently, SAF-3W will provide better lateral beam patterns than SAF-2W(TA) in practical imaging since the term $\sin c^2(\bullet)$ for SAF-3W in (3) is the

result of two-way focusing using a SF technique whereas that for SAF-2W(TA) is obtained from one-way focusing with an effective aperture. It should be also pointed out that SAF-3W provides better lateral resolution than PA(TA), even at z=F (i.e., q=1), when $I = N$; the first term of the right side of (3) has half mainlobe width than that of (5). Since $q = 1$ only at z=F, however, SAF-3W is preferred to PA(TA) even when $I = N/2$. In conclusion, it can be said that SAF-3W is superior to PA(TA) as well as SAF-2W(TA).

If the SNR of PA(RA) is expressed approximately as $10\log(N^2(2N-1))$ for $q = 1$ and $10\log(N(2N-1))$ for $q = 0$, then the SNRs of SAF-2W(RT) and SAF-3W are expected to be $10\log(I(2N-1))$ and $10\log(I \cdot \mu N \cdot N)$, respectively. Notice that $\mu = 1$ in the data acquisition scheme shown in Fig. 2(a), whereas it represents the redundancy factor in the SAF-3W scheme (Fig. 2(b)), whose value depends on N and I with $1/N < \mu < 1$. Hence, in view of SNR, SAF-3W is also better than SAF-2W. One can also increase the SNR of SAF-3W by either using multiple elements to approximately transmit spherical waves or by adopting pulse compression methods.

Computer simulations were performed to verify the theoretical comparison results, using two linear array transducers, both with 192 elements, element spacing of λ, and 60% 6dB bandwidth. In all simulations, the number of transmit and receive subaperture elements will be chosen to be 32 and 64, respectively, unless specified otherwise. Fig. 3 shows the lateral beam patterns of 5MHz linear array for PA(TA) (dashed line), SAF-2W(RA) (thin solid line), and SAF-3W (thick solid line). It is clearly observed that SAF-3W exhibits better beam patterns than the others at all depths. At the transmit focal depth for PA(TA) (z=F=40mm), PA(TA) and SAF-3W must produce the same beam pattern if $I = N/2$, according to (3) and (5). Since $I = N = 32$ for both SAF-2W(RA) and SAF-3W, however, SAF-3W produces smaller mainlobe width and sidelobe levels than PA(TA) as shown in Fig. 3(b). Fig. 3 shows the advantages of three-way focusing (SAF-3W) over two-way focusing (SAF-2W(RA)): the former appears to have slightly larger mainlobe width but much smaller sidelobe levels compared to the latter. All these results are in good agreement with theory.

Fig. 4 shows the lateral beam patterns of a 7.5MHz linear array for PA(RA) (dashed line), SAF-2W(TA) (thin solid line), and SAF-3W (thick solid line), in the presence of phase errors due to tissue inhomogeneity. To mimic tissue imhogeneneity, we simply impose random time delays, with a gaussian distribution, on every data recording from individual element of each receive subaperture: the mean and standard deviation of the time delays are 1.73ns and 22.50ns, respectively. A 32-element receive subaperture is used for PA(RA) in order to make its beam patterns close to those of SAF-3W for comparison purpose.

All the beam patterns are measured at the transmit focal depth for PA(TA) (z=F=30mm). Due to the delay errors, all the plots exhibit unsymmetric beam patterns with fluctuations along the lateral direction and much larger sidelobe levels than those in Fig. 3. In Fig. 4(a), where $I = 0$, SAF-3W and PA(RA) produce the beam patterns that closely resemble each other. Note that they would be identical if it were not for the phase errors. It is important to notice that SAF-2W(TA) for $I = 0$ is most susceptible to phase errors since in this case SAF-2W(TA) reduces to one-way focusing with delay errors.

In Fig. 2(b), where $I = 16$, the peak sidelobe levels of SAF-2W(TA) and SAF-3W are reduced by 13.34dB and 21.24dB, respectively, since the phase errors are averaged while combining different subaperture fields. Particularly, the lateral beam pattern of SAF-2W(TA) becomes much smoother in Fig. 4(b). When I is increased to 32 (Fig. 4(c)), sidelobe levels are further reduced: 6dB mainlobe widths of SAF-3W and SAF-2W(TA) are both reduced by the same factor of 1.4. As can be observed from Fig. 4(c), the differences between the lateral beam patterns of SAF-2W(TA) and SAF-3W are significantly reduced due to the large averaging factor. In practical imaging, it is often inadequate to use large I values because of the motion artifacts. These results demonstrate that SAF-3W is an effective means to improve the lateral resolution of ultrasound imaging.

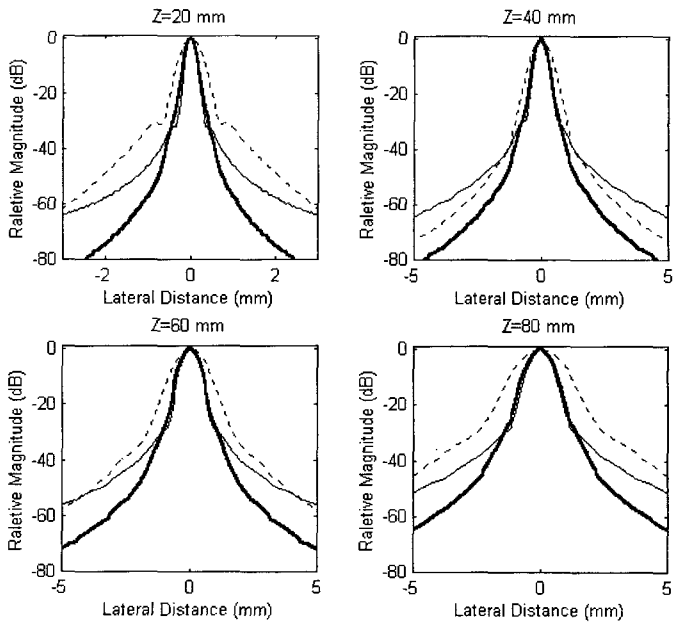

Fig. 3. Comparison of lateral beam patterns of PA (dashed), SAF-2W(RA) (thin solid), and SAF-3W (thick solid) at various depths. In case of PA, ultrasound waves are assumed to be focused at every depth.

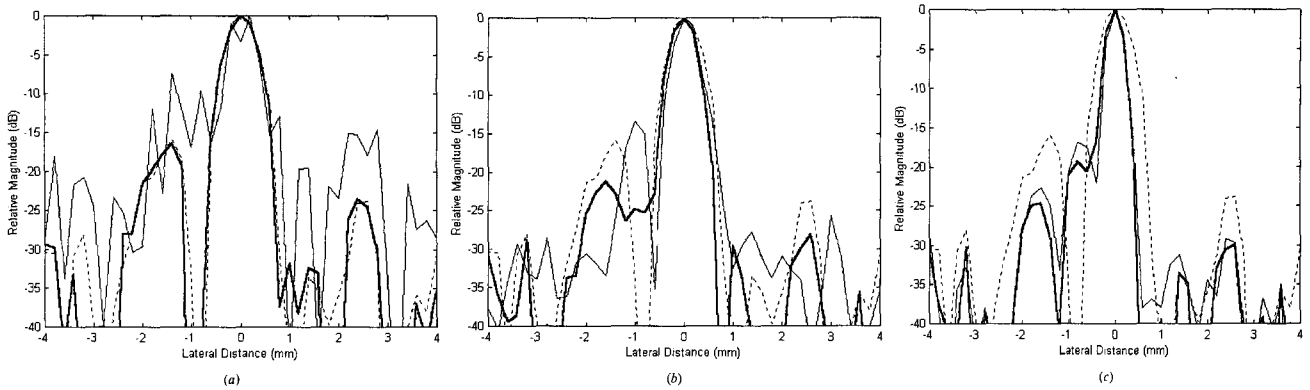

Fig. 4. Lateral beam patterns of PA (dashed), SAF-2W(RA) (thin solid), and SAF-3W (thick solid) at the transmit focal depth of PA (z=F=30mm) for (a) *l*=0, (b) *l*=16, and (c) *l*=32, when random delay errors with gaussian distribution are added to each receiver channel to mimic phase distortions in tissue-like media.

CONCLUSIONS

A three-way dynamic focusing technique was proposed, which can provide better lateral resolution than two-way dynamic focusing methods based on SAF techniques. It was verified through computer simulations as well as theoretical analysis that the proposed method (SAF-3W) produces ultrasound beams with lateral beam patterns represented as the product of the Fourier transforms of the synthetic window function, transmit subaperture, and receive subaperture. Consequently, SAF-3W provides lateral beam patterns with almost the same mainlobe widths but much smaller sidelobe levels than SAF-2W(RA) when both methods are implemented with the same number of receive channels. We also pointed out that in lossless homogenieous media SAF-2W(TA) produces the same three-way beam patterns. In soft tissues, however, SAF-3W outperforms SAF-2W(TA), especially when the number of subapertures used for beam synthesis is small. This is because the product of two focused beam patterns deteriorated due to phase aberrations will result in reduced sidelobe levels compared to those of each beam pattern. Furthermore, SAF-3W can be achieved in real-time by employing a data acquisition scheme which combines a SF method for transmit dynamic focusing and a SAF method for two-way dynamic focusing. From these results, we believe that the proposed method may be very useful for use in imaging slowly moving or stationary objects.

REFERENCES

[1] Levin F. Nock, and Gregg E. Trahey, *"Synthetic Receive Aperture Imaging with Phase Correction for Motion and for Tissue Inhomogeneities-Part : Basic Principles"*, IEEE Trans. Ultrason., Ferroelec., Freq. Contr., Vol. 39, No. 4, pp. 489-495, 1992.

[2] Catherine H. Frazier, and William D. O'Brien, *"Synthetic Aperture Techniques with a Virtual Source Element"*, IEEE Trans. Ultrason., Ferroelec., Freq. Contr., Vol. 45, No. 1, pp. 196-207, 1998.

[3] Mustafa Karaman, and Matthew O'Donnell, *"Synthetic Aperture Imaging for Small Scale Systems"*, IEEE Trans. Ultrason., Ferroelec., Freq. Contr., Vol. 42, No. 3, pp. 429-442, 1995.

[4] Mustafa Karaman, and Matthew O'Donnell, *"Subaperture Processing for Ultrasonic Imaging"*, IEEE Trans. Ultrason., Ferroelec., Freq. Contr., Vol. 45, No. 1, pp. 126-135, 1998.

[5] Richard Y. Chiao, Lewis J. Thomas, and Seth D. Silverstein, *"Sparse Array Imaging with Spatially-Encoded Transmits"*, Proc. IEEE Ultrason. Symp., pp. 1679-1682, 1997.

[6] Moo-Ho Bae, and Mok-Kun Jeong, *"A Study of Synthetic-Aperture Imaging with Virtual Source Elements in B-Mode Ultrasound Imaging Systems"*, IEEE Trans. Ultrason., Ferroelec., Freq. Contr., Vol. 47, No. 6, pp. 1510-1519, 2000.

[7] Geoffrey R. Lockwood, James R. Talman, and Shelby S. Brunke, *"Real-Time 3-D Ultrasound Imaging Using Sparse Synthetic Aperture Beamforming"*, IEEE Trans. Ultrason., Ferroelec., Freq. Contr., Vol. 45, No. 4, pp. 980-988, 1998.

[8] S. W. Flax, and M. O'Donnell, *"Phase-Aberration Correction Using Signals From Point Reflectors and Diffuse Scatterers: Basic Principles"*, IEEE Trans. Ultrason., Ferroelec., Freq. Contr., Vol. 35, No. 6, pp. 758-767, 1988.

[9] Gregg E. Trahey, and Levin F. Nock, *"Synthetic Receive Aperture Imaging with Phase Correction for Motion and for Tissue Inhomogenities-Part : Effects of and Correction for Motion"*, IEEE Trans. Ultrason., Ferroelec., Freq. Contr., Vol. 39, No. 4, pp. 496-501, 1992.

[10] B. D. Steinberg, Principals of Aperture and Array System Design. New York: J. Wiley, 1976.